AIAA AVIATION Forum
22-26 June 2015, Dallas, TX
15th AIAA Aviation Technology, Integration, and Operations Conference

10.2514/6.2015-2701

ERRATA An additional citation had been inadvertently omitted from the original publication (DEC 18, 2015)

Optimal Climb Trajectories Through Explicit Simulation

Timothy T. Takahashi[1]
Arizona State University, Tempe, Arizona, 85281

This paper revisits the famous Rutowski method for shaping lifting ascent trajectories. In this new work, an aircraft-style state variable simulation files many possible ascent trajectories through an explicit series of speed and altitude based waypoints. It examines two aircraft configurations: an A320-like narrow-body airliner powered by turbofan engines and a rocket plane reminiscent of the North American X-15. These configurations highlight the weakness of the Rutowski method and the strengths of using an optimizing aircraft-style explicit state variable simulation to construct high-performance climb procedures.

Nomenclature

ALT	=	Aircraft Flight Altitude (assuming standard day where pressure altitude = altitude above MSL)
CD	=	Drag Coefficient
CL	=	Lift Coefficient
D	=	Drag (lbf)
E	=	Energy
FF	=	Fuel Flow (lbm/hr)
Fs	=	Fuel Specific Energy
He	=	Energy Height (ft)
Kaccel	=	Rate of Climb Correction Factor
KIAS	=	Knots Indicated Airspeed
KTAS	=	Knots True Airspeed
M	=	Mach #
Ps	=	Specific Excess Power: *V (T-D)/W*
Q	=	Dynamic Pressure (lbf/ft^2)
R.O.C.	=	Rate of Climb *(typically ft/min)*
SET	=	Specific Excess Thrust: *(T-D)/W*
T	=	Installed Thrust (lbf)
TSFC	=	Thrust Specific Fuel Consumption (lbm/lbf-hr)
V	=	True Airspeed Velocity (ft/sec)
VKTAS	=	True Airspeed Velocity (nm/hr)
W	=	Weight (lbm)

I. Introduction

FUEL efficiency is an important attribute of many aerospace vehicles. For example, on short range commercial flights, take-off climb burns a significant fraction of total mission fuel. Although fuel burn declines when an aircraft cruises at high altitude, on a short flight the aircraft spends much of its time either ascending or descending. On an hour long flight between Phoenix, AZ and Los Angeles, CA, the aircraft may only spend fifteen minutes of time in level, cruising flight. Takeoff climb might comprise half of the fuel burn for the flight. Reusable fly-back booster space-launch aircraft share many of the same mission characteristics: it must ascend to a high-speed and altitude, it spends only a few moments in level flight where it deploys an upper-stage, before gliding to landing.

[1] Professor of Practice – Aerospace Engineering, School for the Engineering of Matter, Transport and Energy, Arizona State University, Tempe, AZ, 85287. AIAA Associate Fellow.

Combat aircraft experience similar circumstances, where the majority of mission fuel is consumed during its acceleration and climb to a high-altitude, supersonic mission point.

Aircraft performance simulations typically define the flight path by a sequence of commands that is directly intelligible to a pilot. The aircraft must fly at constant indicated airspeed, constant Mach number or constant altitude. The engines may run at a prescribed power setting (such as military power or flight-idle) or throttled back to maintain flight at constant speed and altitude where thrust is in equipoise with drag. While explicit simulations define key trajectory shaping elements such as target altitudes, speeds and distances, other important state variables such as flight path angle or angle-of-attack become implicit byproducts. For example, if thrust exceeds drag, the aircraft can either accelerate or climb. If thrust equals drag, the aircraft will "fly" in steady and level. If thrust is less than drag, the aircraft can decelerate or descend. Whether the aircraft is above or below its target speed or altitude controls whether or not excess thrust is used to accelerate and/or climb. Thus, the explicit simulations derive a speed / altitude profile directly from the state variables used to control its flight.

In contrast, rocket performance simulations traditionally define the flight path by a series of commands that are directly intelligible to a GN&C system but indirectly command speeds, distances and altitudes. Implicit simulation methods successfully define trajectories for ground-to-air missiles as well as large launch vehicles. POST and OTIS, are popular programs that formulate and optimize spacecraft ascent trajectories. OTIS is an acronym for *Optimized Trajectory by Implicit Simulation*.[2] POST is an acronym for *Program to Optimize Simulated Trajectories*.[3] Both of these programs use flight attitudes, like angle of attack (α) or side-slip-angle (β), as their state variables along with throttle position to provide implicitly control of the simulated vehicle trajectory. In other words, they develop an α, β, throttle schedule; they derive the speed / altitude shaping of the flight trajectory from this. This is entirely reasonable from a control theory perspective: we can develop a controller to orient the physical angles at which a vehicle flies.

Unlike pilot-centric explicit simulations, implicit, GN&C based trajectory design does not directly account for the aerodynamics of the vehicle. Implicit simulations, by their choice of state variables, must omit many lessons learned from one hundred plus years of piloted powered flight. In a conventional launch vehicle scenario, this distinction is moot because there is little lift generated by the vehicle. When developing high performance winged vehicles, the choice of implicit simulation state-variables clouds the insight that could otherwise be exploited.

In this paper I explore the bounds of Rutowski's method[1] as a foundation to develop an Optimal Trajectory by Explicit simulation method for high performance vehicle design.

II. Prior Art

In 1954, Rutowski published the original, English language breakthrough on aircraft trajectory design. [1] This seminal work introduced "sky maps," contour plots of performance values presented as a function of Mach and altitude, to develop a minimum time-to-climb and a minimum-fuel-to-climb speed/altitude schedule for aircraft climb. These are explicit definitions of optimal trajectories for climb at a fixed weight. It is a simple, and effective, method to visually understand the flight envelope of a plane, as well as visualize optimum flight conditions. This method was so effective that it is colloquially known as a Rutowski Climb.

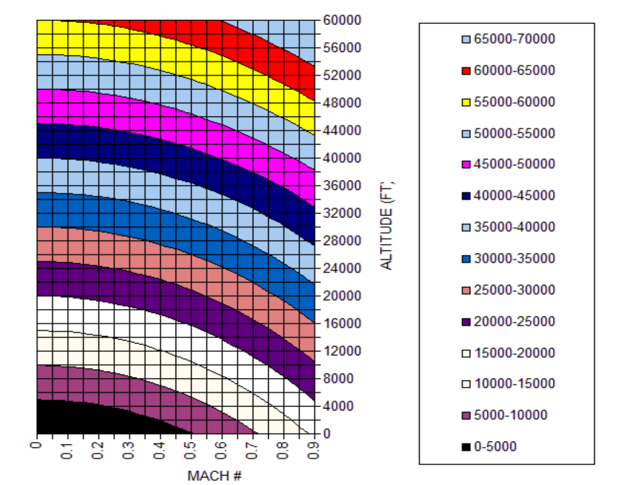

Figure 1 – Contours of Equivalent Energy Height (h_e) as a function of Mach # and Altitude

Rutowski considers the general aircraft performance problem from "the point of view of the balance that must exist between the potential and kinetic energy change of the aircraft, the energy dissipated against the drag, and the energy derived from the fuel."[1] In order to develop an explicit method to finding the speed/altitude schedule to enable a flight of either minimum time or minimum fuel to change from one combination of speed and altitude to another, Rutowski begins by defining the total "energy" of the aircraft as the sum of its mass dependent gravitational potential energy and its kinetic energy:

$$E = W \cdot (ALT + \frac{V^2}{2\,g}) \tag{1}$$

Rutowski's insight to determine the optimal trajectories for climb to a given altitude and speed given minimum time and/or minimum fuel constraints solves a variational calculus problem graphically. The explicitly defined optimal trajectory will attempt to maximize the specific excess power (*Ps)* or fuel specific energy (*Fs*) as the vehicle gains energy height (h_e).

Figure 1 depicts the energy height, h_e. This is the sum of the specific kinetic energy of rigid body motion and the specific potential energy of gravity:

$$h_e = \frac{{V_{KTAS}}^2}{2 \cdot g} + ALT \tag{2}$$

Simply said, the energy height is "the sum of the geometric altitude and the altitude equivalent of the kinetic energy were it all converted into potential energy."[1] For example, 10,000-ft of potential energy height is equivalent to a change in flight speed from rest to ~460 nm/hr.

Rutowski's novation recast fundamental aircraft performance equations in a manner where the altitude, *ALT*, is replaced by the specific energy height, h_e.

In basic aircraft performance, we may compute the specific excess thrust of an airframe using the following equation:

$$SET(M, ALT) = \frac{T(M, ALT) \cdot -D(M, ALT)}{W} \tag{3}$$

Simply said, specific excess thrust is "thrust minus drag over weight." It represents the linear acceleration capability of an airframe. If *SET.=1,* the airframe can accelerate in level flight at a rate of *1 g* (32.2 ft/s^2); it can "stand on its tail" and hover.

The specific excess power, *Ps*, of an airframe is a term closely related to the specific thrust of the aircraft. Recalling from basic physics, the units of power are that of force times length over distance, we can develop a power metric based on the product of the specific excess thrust and the aircraft velocity in knots true airspeed normalized by the weight of the aircraft:

$$P_S(M, ALT) = SET(M, ALT) \cdot VKTAS(M, ALT) \tag{4}$$

If we think about the work-energy theorem from college physics, and make a whole bunch of simplifying assumptions regarding flight at small angles of attack (i.e. the thrust vector is aligned with drag) and climb at small flight path angles (i.e. lift is aligned to oppose weight) we can write the following expression.:

$$(T - D)\, V = W \frac{dALT}{dt} + \frac{W}{g} \frac{d}{dt} (\frac{V^2}{2}) \tag{5}$$

Where *T* is thrust in lbf, *D* is drag in lbf, *V* is velocity in ft/sec, *ALT* is the geopotential altitude of the aircraft in ft, *W* is aircraft mass in lbm, and *g* is the universal gravitational constant (32.2 ft/s^2). In other words, the excess power of the aircraft can translate into a combination of a change in potential energy (change in altitude) or a change in kinetic energy (change in airspeed). The astute reader will note that this equation is only valid on a standard day, where the geopotential altitude exactly corresponds to the pressure altitude.

If we divide Equation 5 through by the weight, W, we get the following expression:

$$P_s = \frac{(T-D)\,V}{W} = \frac{dALT}{dt} + \frac{d}{dt}\left(\frac{V^2}{2g}\right) \qquad (6)$$

In the circumstance where the aircraft performs a constant kinetic energy climb, Equation 6 reduces to:

$$P_s = \frac{(T-D)\,V}{W} = \frac{dALT}{dt} \approx R.O.C._{unaccelerated} \qquad (7)$$

Unfortunately, real aircraft do not always fly truly unaccelerated climb profiles. Piloting convention involves flight at either constant indicated airspeed (KIAS) or constant Mach number (M) for cruise, climbs and descent. During a climb at constant indicated airspeed, the aircraft must increase its kinetic energy as it ascends. Conversely, during a climb at constant Mach number in a region of the atmosphere where there is a cooling temperature gradient with increasing altitude, the aircraft must slightly decrease its kinetic energy as it climbs!

Correction factors, based upon the standard atmosphere, account for this effect.[4]

$$R.O.C(M, ALT) = K_{accel} \cdot R.O.C._{unacellerated}\,(M, ALT) = 101.3\ \cdot K_{accel} \cdot Ps \qquad (8)$$

Because climb at constant indicated airspeed requires the aircraft to physically accelerate and increase its kinetic energy as its climbs, less energy remains to influence changes in potential energy. Thus, an aircraft flying a constant indicated airspeed climb will gain altitude slightly more slowly than the basic, unaccelerated equations of motion would predict. Thus:

$K_{accel} = \dfrac{1}{1+.566816 \cdot M^2}$ for climb at constant KIAS below the tropopause (ALT<36,089-ft), and

$K_{accel} = \dfrac{1}{1+.7 \cdot M^2}$ for climb at constant KIAS above the tropopause (ALT>36,089-ft).

Because climb at constant Mach number will have the aircraft physically, decelerate and lose kinetic energy as its climbs in the tropopause, more energy exists that can influence changes in potential energy. Thus, an aircraft flying a constant Mach number climb in the tropopause will gain altitude slightly more quickly than the basic, unaccelerated equations of motion would predict. Thus:

$K_{accel} = \dfrac{1}{1-.133184 \cdot M^2}$ for climb below the tropopause (ALT<36,089-ft), and,

$K_{accel} = 1$ for climb above the tropopause (ALT>36,089-ft).

Rutowski finds the optimal trajectory for a minimum-time-to-climb ascent to lie along the explicit speed/altitude schedule determined by:

$$\frac{d}{dV_{KTAS}}\left[\frac{T-D}{WT} \cdot V_{KTAS}\right]_{h_e=const} = 0 \qquad (9)$$

for a minimum-time-to-climb flight path.

Rutowski attacked the problem of minimizing the fuel to achieve a speed and altitude using a modified form of the energy method. He introduces a concept known as the Fuel Specific Energy:

$$Fs = \frac{T-D}{WT \cdot TSFC} \cdot V_{KTAS} \qquad (10)$$

He finds the optimal trajectory to lie along the explicit speed/altitude schedule determined by:

$$\frac{d}{dV_{KTAS}}\left[\frac{T-D}{WT \cdot TSFC} \cdot V_{KTAS}\right]_{h_e=const} = 0 \qquad (11)$$

This method is extremely flexible and insightful because it may suggest a "climb with acceleration or even an acceleration in a dive as part of the optimum climb path."[1] Rutowski holds that optimal flight path solutions of this form, which are tedious to find by conventional methods, effortless reveal themselves using his specific energy concept.

The difference between the minimum-fuel-to-climb and the minimum-time-to-climb profile stems from the speed and altitude dependent non-linearities in thrust specific fuel consumption. This nuance is graphically visualized when we examine on contours of *Fs* (which depending upon the engine may more or less closely follow contours of *Ps*). Turbojet engines have little ram drag when compared to high bypass ratio turbofan engines; the *Fs* contours of a turbojet will closely follow *Ps*. Some engines may have a thrust and efficiency lapse that biases the minimum fuel to climb trajectory to higher indicated airspeeds (see Figure 2). Whereas, the very highest bypass-ratio turbofans and open rotor turboprops will have severe thrust and efficiency lapse with airspeed, leading to an *Fs* contour plot with peak values biased towards slower indicated airspeeds.

Subsequent authors Torenbeek,[8] Takahashi[9] and German, Patterson & Takahashi[10] applied Rutowski's graphical process not only to optimum climb trajectories, but also to best altitude and Mach cruise conditions. These are explicit definitions of optimal trajectories (scheduling best speed and best cruise for cruise as a function of weight. It is a simple, and effective, method to visually depict where optimum flight conditions occur.

This study compares and contrasts a direct search for optimal climb performance with elements of the Rutowski climb procedure in order to define a computationally lean method to formulate minimum-fuel-to-climb trajectories for a variety of aerospace vehicles. If a Rutowski inspired method proves highly accurate, it radically simplifies the construction of climb trajectories. Even if Rutowski provides only an approximate starting point for the optimal climb trajectory, it can still simplify the high performance aircraft design process because it bounds the trade space.

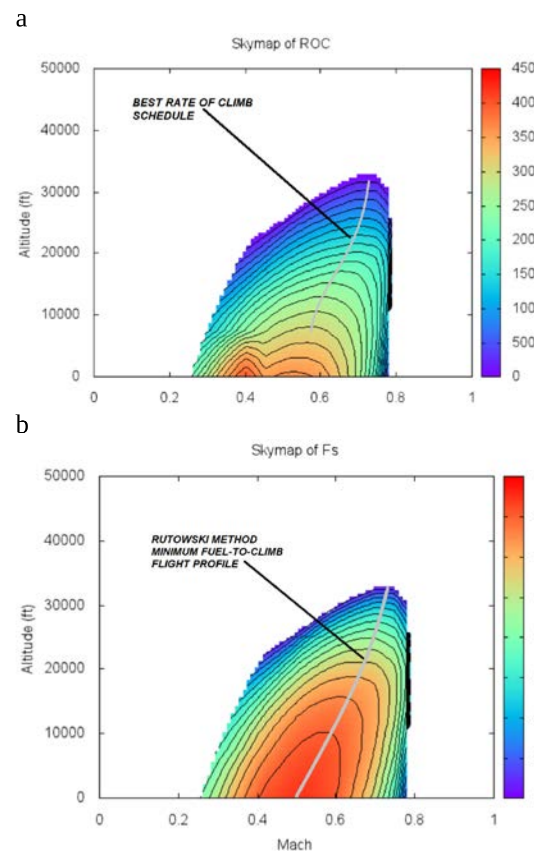

Figure 2 – Skymaps of a) Unaccelerated Rate of Climb and b) Fuel Specific Energy for a notional aircraft.

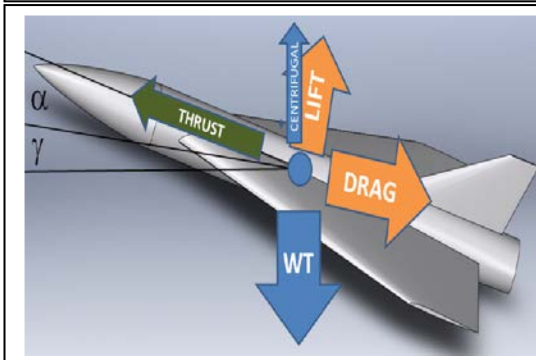

Figure 3 – Free body diagram for Point-Mass Simulation

III. Point Mass Simulation

A point mass simulation of aircraft flight performance facilitates quantitative trade studies. This time-stepping code integrates the basic equations of motion for a lifting flight vehicle flown in a fully inertial reference frame. It implements centripetal forces due to velocities, thus represents trajectories flown over a virtual, cylindrical Earth. This cylindrical Earth model is far simpler to integrate into previously developed aero-performance codes than a spherical Earth model, but does lack the ability for the mission simulations to make changes in inclination. The reduced calculation time and relative simplicity of the model offsets these negatives. In such a model, centrifugal forces oppose gravitational forces in an earth fixed frame. Whereas lift and drag forces reference themselves to a flight-path oriented stability axis reference frame (see Figure 3).

The simulation comprises four basic flight modes:

- steady, level flight at constant Mach number and altitude, where *Thrust* = *Drag*,
- accelerating or decelerating flight at constant altitude given a specified power lever setting,
- climbing or descending flight at constant Mach number given a specified power lever setting, and
- climbing or descending flight at constant indicated airspeed given a specified power lever setting.

The aerodynamics model used in these simulations derives from a prepared database of lift and drag data based upon the following decomposition:

$$L = CL(M, \alpha) \cdot q \cdot Sref \quad (12)$$
$$D = [CD(M, \alpha) + \Delta CD0(M, ALT)] \cdot q \cdot Sref \quad (13)$$

Where *CL*, *CD* and *ΔCD0* are tables of data; *q* is the dynamic pressure of flight derived from the standard atmosphere and *Sref* is the wing planform reference area. The nominal drag polars $CD(M,\alpha)$ represent flight at a specific reference altitude. The Reynolds Number correction term: *ΔCD0(M,ALT)* represents changes in surface skin friction that occurs when the aircraft flies above or below the reference altitude.

The propulsion model used in these simulations derives from a prepared database of "five column" performance data (thrust and thrust-specific-fuel-consumption as a function of Mach number, altitude and power code):

$$T = THRUST(M, ALT, PLA) \quad (14)$$
$$FF = THRUST(M, ALT, PLA) \cdot TSFC(M, ALT, PLA) \quad (15)$$

Where *THRUST(M,ALT,PLA)* and *TSFC(M,ALT,PLA)* represent the five columns of tabular data. THRUST is given in units of pounds force. *TSFC* being express in terms of pounds mass of fuel burned per pound force of thrust per hour. *PLA* represents a power lever angle that varies from 0.0 with the engine off through 1.0 with the engine at full power.

This simulation will be used as the basis of the trade studies found in Sections IV and V of this manuscript.

IV. Trade Studies – Narrow Body Airliner (generic A320-inspired model)

This first study comprises a collection of simulation results for a generic Airbus A320-like configuration. It simulates take-off departure procedures. In the first instance, simulations begin at a brake release weight of W=150,000-lbm and climb up to an initial cruise speed of Mach 0.80 at ALT=36,000-ft. In the second instance, the process repeats process but with a brake release weight of W=100,000-lbm. In this sense, the study can encompass changes in both thrust loading (T/W) and wing loading (W/S).

In order to estimate lift and drag, an

Ps	0.30	0.32	0.34	0.36	0.38	0.40	0.42	0.44	0.46	0.48	0.50	0.52	0.54	0.56	0.58	0.60	0.62	0.64	0.66	0.68	0.70	0.72	0.74	0.76	0.78	0.80
40000																								0.3	0.8	0.7
38000																				1.2	2.2	3.0	3.5	3.4	4.2	4.1
36000																	1.5	3.1	4.3	5.1	5.6	6.2	6.9	6.9	6.9	6.7
34000															0.8	4.2	5.6	6.6	7.6	8.4	8.9	8.9	9.5	9.3	9.1	8.6
32000														4.5	6.5	8.0	9.0	9.6	10.1	10.9	11.3	11.1	11.2	10.8	10.5	9.8
30000												0.5	7.2	9.0	10.1	11.0	11.9	12.5	12.7	13.0	13.2	12.7	12.8	12.1	11.9	10.8
28000											3.8	9.3	10.7	11.6	12.6	13.6	14.3	14.8	14.8	14.7	14.8	14.2	14.2	13.6	12.8	12.0
26000										6.3	10.9	12.3	13.7	14.7	15.4	15.7	16.4	16.6	16.4	16.4	16.1	15.9	15.2	14.7	13.5	12.6
24000									8.2	12.5	14.2	15.5	16.5	17.2	17.7	17.9	18.2	18.2	17.8	17.9	17.3	17.0	16.3	15.4	14.6	13.1
22000								9.4	14.0	15.8	17.1	18.1	18.9	19.5	19.7	19.7	19.9	19.6	19.6	19.0	18.7	17.6	17.1	16.2	14.6	13.1
20000							10.0	15.4	17.2	18.6	19.5	20.4	21.1	21.4	21.2	21.4	21.4	21.1	20.8	20.2	19.5	18.9	17.6	16.4	14.9	12.9
18000						9.9	16.7	18.4	20.0	21.0	21.8	22.6	22.9	22.9	22.9	23.1	22.6	22.5	21.6	21.3	20.4	19.1	17.9	16.3	14.3	12.1
16000					8.9	17.7	19.6	21.2	22.4	23.3	24.0	24.4	24.6	24.4	24.7	24.3	24.1	23.4	22.9	21.9	20.8	19.6	17.8	15.8	13.8	11.2
14000				6.4	18.1	20.8	22.3	23.7	24.6	25.5	25.8	26.1	26.0	26.2	26.0	25.6	25.1	24.6	23.2	22.3	21.0	19.1	17.6	15.3	12.7	9.6
12000			2.1	17.5	21.5	23.1	24.8	25.9	26.8	27.3	27.5	27.5	27.7	27.5	27.1	26.7	26.0	24.8	23.8	22.4	20.6	18.9	16.8	14.2	11.1	7.6
10000			15.2	22.1	24.3	25.5	27.0	28.1	28.6	29.0	28.9	29.2	29.1	28.6	28.3	27.5	26.5	25.4	23.9	22.1	20.3	18.1	15.6	12.6	9.2	5.3
8000		13.8	25.6	28.0	30.1	31.4	32.1	32.2	31.9	31.0	30.5	30.4	30.0	29.7	28.9	28.0	26.9	25.2	23.6	21.7	19.4	16.6	13.6	10.7	6.9	2.5
6000	9.1	26.8	31.7	33.9	35.8	37.1	37.0	36.2	34.9	33.7	31.8	31.4	31.2	30.4	29.6	28.4	26.7	25.1	23.2	20.8	18.2	15.2	11.9	8.5	4.4	
4000	23.7	33.2	36.0	38.2	40.0	41.4	40.4	39.2	37.6	36.4	32.7	32.6	31.8	31.0	29.8	28.3	26.7	24.7	22.3	19.6	16.8	13.5	9.8	6.0	1.5	
2000	32.2	36.2	38.9	40.9	42.7	43.9	42.8	41.3	39.1	36.6	33.8	33.1	32.4	31.2	29.7	28.3	26.3	23.9	21.2	18.3	16.1	11.4	7.6	3.3		
0	36.0	39.0	41.6	43.5	45.2	46.3	44.9	42.9	40.7	37.9	34.6	33.8	32.7	31.2	29.8	27.9	25.6	22.9	20.0	16.7	13.2	9.2	4.8	0.2		

a

Ps	0.30	0.32	0.34	0.36	0.38	0.40	0.42	0.44	0.46	0.48	0.50	0.52	0.54	0.56	0.58	0.60	0.62	0.64	0.66	0.68	0.70	0.72	0.74	0.76	0.78	0.80
40000													2.11	7.85	9.47	10.6	11.6	12.5	13.1	13.3	14	14.1	13.7	13.9	13.2	13
38000												7.28	10.9	12.4	13.6	14.6	15.3	16.3	17	17.2	17.3	17.4	17.1	17.1	16.6	15.9
36000										1.41	11.3	14	15.7	17	18	18.8	19.4	19.9	20.4	20.4	20.6	20.5	20.4	19.9	19.6	18.6
34000									5.58	14.5	16.9	18.3	19.5	20.5	21.5	22.3	22.7	22.9	23.3	23	23.5	22.9	23	22.3	21.7	21.
32000								8.47	17	19.1	20.3	21.6	22.7	23.5	24.5	25.1	25.2	25.4	25.6	25.5	25.4	25.1	24.4	24.1	23.2	21.8
30000							10.4	19	21.1	22.5	23.9	25.1	26	26.6	27.2	27.6	27.5	27.9	27.7	27.7	27	26.9	26.2	25.1	24.2	22.6
28000						11.4	20.7	23	24.5	26	27.2	28.2	28.8	29.1	29.7	29.9	30	30	29.7	29.4	29.1	28.2	27.3	26.2	24.8	22.8
26000					11.6	22.1	24.7	26.3	27.9	29.2	30.2	30.9	31.2	31.7	32.1	31.9	32.2	31.7	31.7	31.1	30.3	29.5	28.3	26.6	25.1	23
24000				10.4	23	26.2	27.9	29.7	31	32.1	32.8	33.3	33.6	34.2	34.2	34.3	34	33.9	33.1	32.4	31.6	30.2	29	27.3	25.3	22.7
22000			7.51	23	27.4	29.4	31.2	32.7	33.9	34.7	35.2	35.6	36.2	36.3	36.3	36.2	35.9	35.2	34.7	33.7	32.3	31.1	29.5	27.4	24.9	22
20000		2.52	21.8	28.4	30.9	32.5	34.2	35.6	36.5	37.1	37.5	38.1	38.4	38.3	38.3	38	37.5	36.8	35.7	34.5	33.2	31.5	29.5	27.1	24.3	20.9
18000		18.8	29.4	31.9	33.9	35.6	37.1	38.2	39	39.4	40	40.4	40.2	40.5	40.1	39.7	39	37.7	36.7	35.3	33.5	31.3	28.8	26.3	23.2	19.3
16000	13.3	28.8	32.9	35.1	36.8	38.4	39.7	40.6	41.2	41.9	42.3	42.2	42.6	42.1	41.9	41.1	40.1	39	37.5	35.7	33.6	31.1	28.2	25.3	21.7	17.3
14000	26.1	33	35.8	38.1	39.6	41.1	42.1	42.8	43.8	44.3	44.2	44.6	44.3	44	43.2	42.3	41.2	39.7	37.8	35.7	33.3	30.4	27.2	23.9	19.8	14.8
12000	33.4	36.6	38.8	41	42.5	43.5	44.6	45.6	46.1	46.3	46.6	46.3	46.1	45.3	44.5	43.4	41.9	39.9	37.8	35.3	32.6	29.4	25.8	21.9	17.3	11.8
10000	36.9	39.6	41.7	43.7	45.1	46.1	47.2	47.9	48.1	48.6	48.3	48.2	47.5	46.7	45.6	44.1	42.2	40.1	37.6	34.8	31.7	28	24	19.7	14.4	8.29
8000	44	46.9	49.1	51.2	52.7	54	54	53.5	52.9	51.4	50	49.4	48.6	47.6	46.1	44.3	42.2	39.7	36.8	33.7	30.2	26.1	21.6	16.7	10.9	4.14
6000	51	54.1	56.5	58.5	60.3	61.7	60.8	59.4	57.1	54.6	51.3	50.6	49.6	48.2	46.4	44.4	41.9	39.1	35.9	32.3	28.4	23.8	18.9	13.4	7.04	
4000	56.3	59.4	61.9	63.9	65.9	67.4	65.7	63.3	60.4	56.7	52.5	51.6	50.2	48.5	46.5	44.1	41.3	38.1	34.5	30.5	26.2	21.2	15.7	9.69	2.67	
2000	59.7	62.7	65.2	67.4	69.2	70.5	68.6	65.8	62.3	58.2	53.4	52.1	50.5	48.5	46.2	43.6	40.4	36.8	32.9	28.4	23.6	18.1	12.1	5.49		
0	63.2	65.8	68.4	70.5	72.2	73.8	71.2	68.1	64.1	59.5	54.1	52.5	50.7	48.4	45.8	42.8	39.3	35.3	30.9	26	20.7	14.7	8.13	0.88		

b

Figure 4 – Specific Excess Power (*Ps*) Grid for narrow body transport configuration. a) W=150,000-lbm, b) W=100,000-lbm

aerodynamic model of the A320 was developed from published sketches, photographs and dimensions that determine from wetted areas, planform areas, and thickness. The aerodynamic model was built using EDET, a code developed by NASA and Lockheed-California during the mid 1970's.[5]

Five column propulsion data was prepared using the NASA developed NPSS program.[6] NPSS simulates an engine with a reference bypass ratio of 6:1, a design-point operating overall pressure ratio (OPR) of 27.5, a maximum turbine inlet temperature of 2,500°F and a design-point fan-pressure-ratio of 1.6. The computed installed propulsion performance assumes a reference inlet recovery efficiency of 99.5%, a design-point fan efficiency of 85%, a design-point low-pressure-compressor-spool efficiency of 85%, and a design-point high-pressure-compressor-spool efficiency of 85%. The design point burner efficiency was set to 87%; the high-pressure exhaust turbine spool efficiency was set to 87%.

The section compares and contrasts the following departure and climb out procedures that are compatible with US air traffic control regulations. [7]

Trade Study Procedure # 1:

1. Begin at ALT=400-ft, 200 KIAS
2. Acceleration to *x* KIAS, not to exceed 250 KIAS
3. Initial climb at constant KIAS to ALT=10,000-ft
4. If initial climb limited to 250 KIAS, then accelerate to *x* KIAS at ALT=10,000-ft
5. Climb at constant KIAS until M=0.8 or ALT=36,000-ft is attained
6. Climb at constant Mach number until ALT=36,000-ft is attained

a

Fs	0.30	0.32	0.34	0.36	0.38	0.40	0.42	0.44	0.46	0.48	0.50	0.52	0.54	0.56	0.58	0.60	0.62	0.64	0.66	0.68	0.70	0.72	0.74	0.76	0.78	0.80
40000																								0.4	1.4	1.1
38000																				2.1	3.8	5.1	5.9	5.8	7.0	6.7
36000																	2.8	5.6	7.6	9.0	9.7	10.8	11.8	11.6	11.6	11.1
34000															1.5	7.8	10.2	12.0	13.6	14.8	15.6	15.4	16.2	15.8	15.1	14.2
32000														8.6	12.2	14.8	16.4	17.4	18.0	19.2	19.8	19.2	19.1	18.3	17.6	16.2
30000												0.9	14.0	17.1	19.0	20.5	21.8	22.6	22.7	23.0	23.0	21.9	21.9	20.4	19.8	17.7
28000											7.5	18.1	20.7	22.1	23.5	25.0	26.1	26.7	26.4	26.0	25.7	24.5	24.1	22.7	21.3	19.7
26000										12.7	21.7	24.2	26.4	28.0	28.9	29.1	30.1	30.1	29.2	29.0	28.0	27.2	25.8	24.7	22.4	20.6
24000									16.8	26.2	28.1	30.4	31.9	32.8	33.2	33.1	33.4	32.9	31.8	31.5	30.0	29.1	27.5	25.7	24.0	21.2
22000								19.6	28.6	31.8	33.9	35.4	36.4	37.0	37.0	36.4	36.3	35.2	34.7	33.3	32.2	30.0	28.8	26.8	24.0	21.2
20000							21.2	32.1	35.2	37.5	38.8	39.8	40.6	40.6	39.7	39.5	38.9	37.8	36.8	35.2	33.5	32.0	29.5	27.0	24.3	20.7
18000						21.2	35.4	38.3	40.9	42.3	43.2	44.1	44.1	43.4	42.7	42.4	40.8	40.1	38.0	36.9	34.9	32.2	29.8	26.8	23.1	19.2
16000					19.4	38.0	41.1	44.1	45.7	46.7	47.5	47.5	47.0	46.0	45.9	44.5	43.4	41.5	40.1	37.7	35.4	32.6	29.3	25.7	22.1	17.6
14000				14.2	39.5	44.4	46.9	49.0	50.2	51.0	50.9	50.5	49.5	49.3	48.0	46.6	44.9	43.2	40.3	38.2	35.4	31.8	28.6	24.7	20.3	15.1
12000			4.6	38.7	46.9	49.4	52.0	53.5	54.4	54.4	53.9	53.0	52.6	51.4	49.8	48.2	46.2	43.5	41.1	38.0	34.5	31.0	27.2	22.7	17.5	11.7
10000			34.3	48.9	52.8	54.3	56.6	57.8	58.0	57.6	56.5	56.1	55.0	53.2	51.6	49.4	46.9	44.3	40.9	37.2	33.7	29.6	25.1	19.9	14.4	8.1
8000		31.0	56.5	60.8	64.1	65.7	66.3	65.5	63.8	61.2	59.2	58.1	56.2	54.8	52.4	49.9	47.1	43.5	40.0	36.1	31.8	26.8	21.7	16.7	10.7	3.8
6000	20.5	59.3	69.0	72.5	75.2	76.5	75.4	72.8	69.4	66.0	61.3	59.5	58.1	56.6	53.2	50.1	46.4	43.0	39.0	34.4	29.5	24.2	18.7	13.2	6.6	
4000	53.0	73.0	77.8	81.0	83.4	84.7	81.9	78.4	74.3	68.9	62.6	61.3	58.8	56.3	53.2	49.5	46.0	41.8	37.1	32.1	26.9	21.3	15.3	9.2	2.2	
2000	72.0	79.6	83.8	86.7	88.8	89.7	86.3	82.2	78.8	70.7	64.2	61.8	59.3	56.2	52.5	49.0	44.8	40.0	34.9	29.5	23.9	17.9	11.5	4.9		
0	80.3	85.4	89.6	91.9	93.7	94.2	90.2	85.1	79.4	72.8	65.1	62.5	59.4	56.7	52.1	47.9	43.0	37.9	32.5	26.7	20.7	14.2	7.4	0.3		

b

Fs	0.30	0.32	0.34	0.36	0.38	0.40	0.42	0.44	0.46	0.48	0.50	0.52	0.54	0.56	0.58	0.60	0.62	0.64	0.66	0.68	0.70	0.72	0.74	0.76	0.78	0.80
40000													4.01	14.8	17.6	19.4	21	22.4	23.4	23.5	24.3	24.3	23.4	23.5	22	21.6
38000												14	20.7	23.3	25.3	26.8	27.9	29.4	30.3	30.2	30.2	30.1	29.3	28.8	27.8	26.3
36000										2.78	22.1	26.9	30	31.9	33.5	34.6	35.2	35.8	36.3	36	36	35.4	34.9	33.6	32.8	30.8
34000									11.2	28.8	33	35.4	37.2	38.8	40.1	41.1	41.4	41.2	41.6	40.6	41	39.6	39.3	37.7	36.3	34.7
32000								17.4	34.3	38.1	39.9	42	43.6	44.5	45.9	46.4	46.1	45.9	45.8	45.1	44.4	43.3	41.7	40.7	38.7	36
30000							21.7	39.1	42.9	45	47.3	49	50	50.6	51.1	51.2	50.4	50.6	49.5	49	47.2	46.4	44.8	42.4	40.3	37.3
28000						24.2	43.4	47.5	50	52.3	53.8	55.1	55.6	55.3	55.8	55.5	55	54.3	53.1	51.9	50.7	48.5	46.5	44.1	41.1	37.5
26000					25.2	47.2	52.1	54.6	57.2	58.8	59.9	60.5	60.3	60.3	60.4	59.3	59	57.3	56.6	54.9	52.7	50.6	47.9	44.6	41.6	37.7
24000				23	50	56.2	58.8	61.7	63.5	64.8	65.2	65.2	64.8	65.2	64.2	63.5	62.1	61.1	58.9	57	54.8	51.7	48.9	45.6	41.7	37
22000			17	51	59.8	63.1	66	68.1	69.5	70	70	69.6	69.8	69.1	68	66.9	65.5	63.3	61.5	58.9	55.8	52.9	49.6	45.6	40.9	35.5
20000		5.79	49.2	63.2	67.6	69.7	72.4	74.1	74.8	74.9	74.4	74.5	74	72.6	71.7	70	68.1	66	63.2	60.1	57	53.5	49.4	44.7	39.6	33.7
18000		43.1	66.5	71	74	76.3	78.4	79.4	79.7	79.2	79.1	78.7	77.3	76.6	74.6	72.8	70.5	67.3	64.5	61.1	57.3	52.7	47.9	43.2	37.4	30.8
16000	31.1	66.4	74.4	78.1	80.3	82.4	83.8	84.4	84.1	84.2	83.5	82.1	81.6	79.4	77.8	75.2	72.1	69.2	65.6	61.5	57	52	46.6	41.3	34.8	27.4
14000	61	75.9	80.8	84.6	86.4	87.9	88.7	88.7	89.2	88.6	87	86.5	84.4	82.6	79.9	76.9	73.8	70	65.6	61	56.1	50.6	44.6	38.5	31.4	23.2
12000	78.1	84	87.5	90.8	92.4	93	93.6	94.1	93.6	92.3	91.3	89.3	87.5	84.6	81.6	78.4	74.5	69.9	65.2	60	54.5	48.4	41.8	35	27.2	18.2
10000	86.1	90.9	94	96.8	97.9	98.3	98.9	98.6	97.4	96.7	94.4	92.6	89.7	86.7	83.3	79.3	74.7	69.7	64.4	58.7	52.5	45.8	38.6	31.1	22.5	12.7
8000	101	105	108	111	112	113	111	109	106	101	97	94.2	91.2	87.7	83.5	78.9	73.8	68.4	62.5	56.1	49.5	42.1	34.3	26.2	16.9	6.28
6000	115	120	123	125	127	127	124	120	113	107	98.9	96	92.5	88.2	83.5	78.4	72.8	66.7	60.3	53.3	46	38.1	29.7	20.8	10.7	
4000	126	131	134	136	137	138	133	127	119	110	101	97.1	92.8	88	82.8	77.2	71.1	64.5	57.4	49.9	42	33.5	24.4	14.8	4.02	
2000	133	138	141	143	144	144	138	131	122	112	101	97.2	92.5	87.3	81.6	75.5	68.8	61.7	54	45.9	37.4	28.3	18.6	8.3		
0	141	144	147	149	150	150	143	135	125	114	102	97.2	92	86.3	80.1	73.5	66.3	58.5	50.3	41.6	32.4	22.7	12.3	1.31		

Figure 5 – Fuel Specific Energy (*Fs*) Grid for narrow body transport configuration. a) W=150,000-lbm, b) W=100,000-lbm

Climb Schedule (ALT)	150000-LBM		100000-LBM	
	MinTime	MinFuel	MinTime	MinFuel
36000	M=0.74	243	M=.80	215
34000	M=0.74	243	M=.80	215
32000	M=0.74	243	M=.66	215
30000	252	243	M=.66	215
28000	252	243	245	215
26000	252	243	245	215
24000	252	243	245	215
22000	252	243	M=.58	215
20000	252	243	M=.58	215
18000	263	243	263	215
16000	263	243	263	M=0.44
14000	263	243	263	M=0.44
12000	263	250	263	230
10000	263	250	263	230
8000	250	250	M=0.4	M=0.4
6000	250	250	M=0.4	M=0.4
4000	250	250	M=0.4	M=0.4
2000	250	250	M=0.4	M=0.4
0	250	250	250	250

Figure 6 – Rutowski Procedure Climb Speed Schedule for Narrow Body Transport

Trade Study Procedure # 2:

`Follow Rutowski Minimum-Fuel-To-Climb procedure, airspeeds not to exceed 250KIAS below 10,000-ft`

and

Trade Study Procedure # 3:

`Follow Rutowski Minimum-Time-To-Climb procedure, , airspeeds not to exceed 250KIAS below 10,000-ft`

The Rutowski speed schedules were determined through the development of *Ps* and *Fs* skymap charts for our notional airliner. Figures 4 and 5 comprise respective grids of *Ps* and *Fs* values as a function of standard day altitude and Mach number at flight weighs of *W*=150,000-lbm and *W*=100,000-lbm. As the aircraft flight weight decreases, both *Ps* and *Fs* increase. Recall that this phenomenon exists because 1) maximum thrust is not a function of flight weight, 2) TSFC at maximum thrust is not a function of flight weight, 3) increased flight weight leads to higher dimensional drag at any particular speed / altitude combination and that 4) increased flight weight appears in the denominator of both *Ps* and *Fs*. These grids highlight the peak values of *Ps* and *Fs* at each altitude; together they define the explicit accelerate / climb procedure from take-off to cruise.

In an ideal world, Rutowski encourages aircraft to both fly faster than the U.S. Air Traffic Control low altitude speed limit permits (not to exceed 250 KIAS below 10,000-ft) and overshoot the target altitude at a slow climb speed and "power dive" to attain final cruise altitudes. These potential artifacts were removed in order to determine a flyable Rutowski inspired climb speed schedule. In addition, the locus of Rutowski method target points in Mach / altitude space may be transformed wherever practicable into a more pilot (and simulation) friendly Mach / indicated airspeed schedule. Figure 6 depicts these climb profiles, with speeds smoothed and rounded to the nearest 2 knots or 0.01 Mach number.

The results of these trades are interesting.

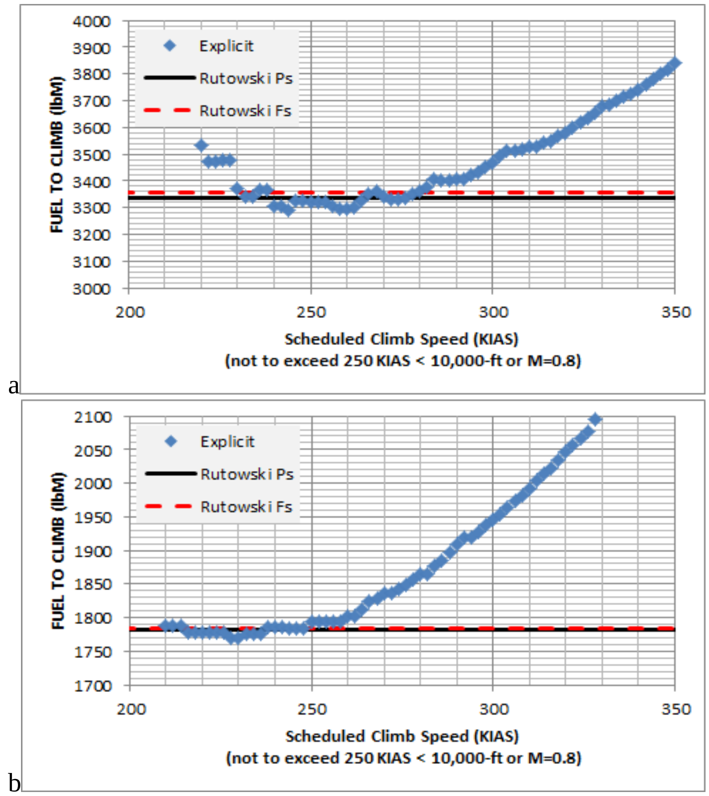

Figure 7 – Fuel to Climb for Narrow Body transport configuration. a) W=150,000-lbm, b) W=100,000-lbm

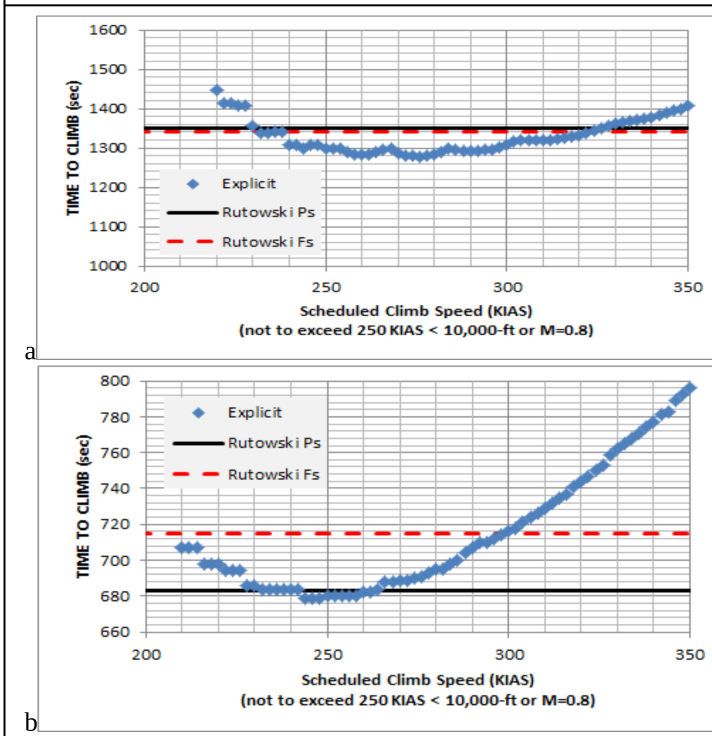

Figure 8 – Time to Climb for Narrow Body transport configuration. a) W=150,000-lbm, b) W=100,000-lbm

Figure 7 compares and contrasts the fuel consumption for the aforementioned climb procedures. Interestingly, for both studied cases the Rutowski Minimum-Time-To-Climb speed schedule produced slightly lower fuel consumption than the Rutowski Minimum-Fuel-To-Climb speed schedule. More interestingly, the best climb profiles developed using the simplified Procedure # 1 method could produce an ascent trajectory that was slightly (but not significantly) more efficient than Rutowski. The most efficient climb at W=150,000-lbm had the aircraft climb at ~245 KIAS all the way up to the final cruise altitude. The most efficient climb at W=100,000-lbm has the aircraft climb at ~230 KIAS all the way up the final cruise altitudes. These optimized speed schedules are similar (but slightly slower) to those selected by the Rutowski algorithm. Unlike Rutowski, the point-mass-simulation includes corrections for large-angles of attack and flight path angles, so we might expect the "best solution" to differ slightly. To summarize, the Rutowski procedure develops a plausible and competitive flight path schedule to explicitly define a climb profile.

Figure 8 compares and contrasts the time to climb implied by these climb procedures. The fastest times to climb, interestingly, arise from use of Procedure # 1. At the same time, the Rutowski Minimum Time-to-Climb procedure produced competitive results. In either case, the optimized speed schedules are similar to those selected by the Rutowski algorithm. As with the minimum fuel-to-climb procedure, Rutowski's method develops a plausible and competitive flight path schedule to explicitly define climb. However, an optimizer running an explicit flight trajectory simulation may find slight improvements upon Rutowski.

When looking at the results, one may ask whether the respective contours of Ps and Fs used by Rutowski procedure are qualitatively or quantitatively useful. As flight weight decreases, *Ps* and *Fs* increase; at the same time, the time-to-climb and fuel-to-climb decreases. Is there causality?

In the case of time-to-climb, the causality is directly attributable to the magnitude of *Ps*. The units of *Ps* are distance per unit time. Because *Ps* directly represents the unaccelerated rate of climb, doubling *Ps* will essentially half the time required to climb from one altitude to another.

In the case of fuel-to-climb, the causality is less clear. *Fs* is neither dimensionless, nor a representation of mass per unit distance, its units are distance. Nonetheless, the question remains whether all attributes that lead to an increase *Fs* reduce the amount of fuel needed to climb.

Figure 9 compares the fuel burn for the reference narrow body aircraft with three engine options: the nominal engine, a 90% thrust version (a 10% reduction in thrust across the entire flight envelope) and a 110% thrust version (a 10% increase in thrust across the entire flight envelope). The derated engines result in lower values of *Fs* across the entire envelope, they also lead to substantially increased fuel burn in climb. Conversely, the oversized engines correspond to an aircraft with greater *Fs* that burns substantially less fuel in climb. Moreover, the indicated airspeed corresponding to the minimum fuel burn climb increases slightly with increasing engine capacity. Contrary to expectation that larger engines will always burn more fuel, the reader can see that larger engines lead to lower overall fuel burns, a faster rate of climb and an optimum climb at a higher indicated airspeed. In this example, a 10% reduction in thrust leads to a 12% increase in fuel burn even while taking into account the revised optimum climb speed.

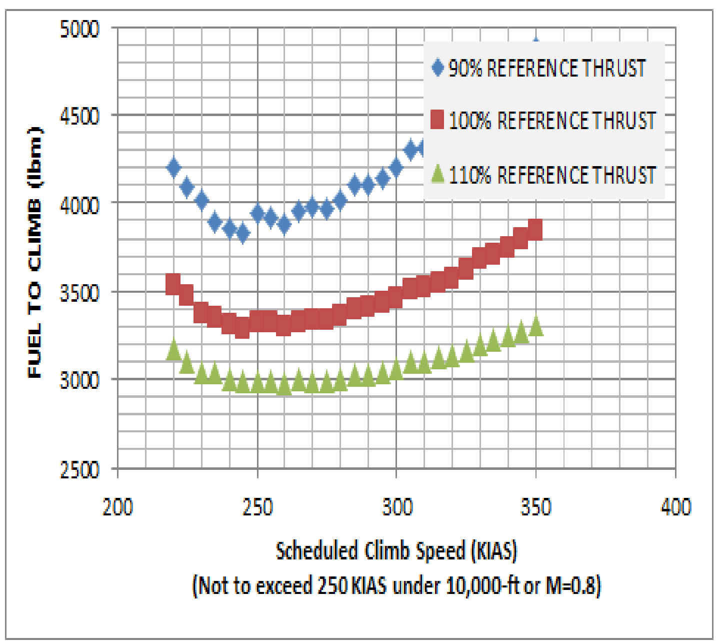

Figure 9 – Fuel to Climb for Narrow Body transport configuration. W=150,000-lbm. Various Thrust Loadings.

V. Trade Studies – Air Launched Rocket Plane (X-15)

The second study comprises a collection of simulation results for a best estimate of the North American X-15 rocket plane. In an access to space launch simulation, flight begins with an air drop at W=33,000-lbm at Mach 0.8 and ALT=40,000-ft. The liquid fuel rocket engine will then ignite. The aircraft will accelerate and climb to eventually reach a speed of Mach 4.5 at ALT=105,000-ft. At this point, the aircraft would launch an upper stage and then glide back and land at a friendly runway.

In order to estimate lift and drag, an aerodynamic model of the X-15 was developed by Mr. Gaines Gibson using published wind tunnel[11,12,13] and flight test data.[14] (see Errata Ref. 18) Similarly, rocket propulsion data representing the XLR-99 was developed from a mix of open source data[15] and thermodynamic first principles. [16,17]

The section compares and contrasts the following ascent procedures:

Trade Study Procedure # 1:

1. Begin at ALT=40,000-ft, M=0.8
2. Level acceleration to M=y at ALT=40,000-ft
3. Climb at constant KIAS to ALT=105,000-ft, not to exceed M=4.5
4. Accelerate at ALT=105,000-ft to M=4.5

Figure 10 – Fuel Specific Energy (*Fs*) Grid for X-15 at W=33,000-lbm

Figure 11 – Specific Excess Power (*Ps*) Grid for X-15 at W=33,000-lbm.

Trade Study Procedure # 2 uses the locus of peak *Fs* points found at discrete energy heights from Figure 10 to determine the Rutowski minimum fuel-to-climb procedure. In this case, the profile can be represented as:

1. Begin at ALT=40,000-ft, M=0.8
2. Level acceleration to 875 KIAS at ALT=40,000-ft at full power
3. Climb at constant KIAS to ALT=56,000-ft, not to exceed M=4.5
4. Climb at constant Mach # to ALT=105,000-ft at M=4.5

Trade Study Procedure # 3 uses the locus of peak *Ps* points found at discrete energy heights from Figure 11 to determine the Rutowski minimum time-to-climb procedure. In this case, the profile can be represented as:

1. Begin at ALT=40,000-ft, M=0.8
2. Level acceleration to 950 KIAS at ALT=40,000-ft at full power
3. Climb at constant KIAS to ALT=50,000-ft, not to exceed M=4.5
4. Climb at constant Mach # to ALT=105,000-ft at M=4.5

The results of these trades are even more interesting than those found for the narrow body airliner.

Figures 12 and 13 compare and contrast the fuel consumption and engine burn times for the aforementioned three ascent trajectories. As with the airliner model, simulations following the Rutowski Minimum-Time-To-Climb speed schedule consumed slightly less fuel consumption than those following the Rutowski Minimum-Fuel-To-Climb speed schedule. Again, the best climb profiles developed using the simplified Procedure # 1 method produced ascent trajectories that were more efficient than Rutowski. In this case, the optimum trajectory suggested through explicit simulation differs sharply from the Rutowski profile. The optimizer suggests a brief acceleration through the transonic. A constant indicated airspeed begins at Mach 1.5 (450 KIAS), which has the aircraft attain Mach 4.5 at 86,000-ft. The final segment of the ascent trajectory involves a constant Mach number climb to 105,000-ft. Conversely, the Rutowski methods both suggest a significant level acceleration stage at 40,000-ft, followed by a much shorter constant indicated airspeed climb segment. Rutowski holds the aircraft low in the atmosphere longer resulting in greater fuel consumption and longer times to climb than the optimal trajectories found by implicit simulations. The difference in fuel consumption is marked, the choice of trajectory can lead to nearly 2000-lbm savings out of a potential fuel load of 14,000-lbm (~15%).

Figure 14 documents the flight path of the optimum ascent trajectory attained through the optimizing explicit simulation. The flight path angle is zero degrees during the level acceleration through the transonic.

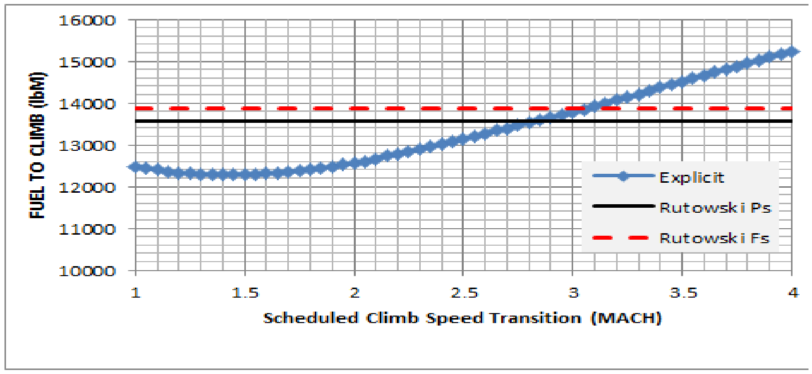

Figure 12 – Fuel to Climb for X-15 Rocket plane configuration.

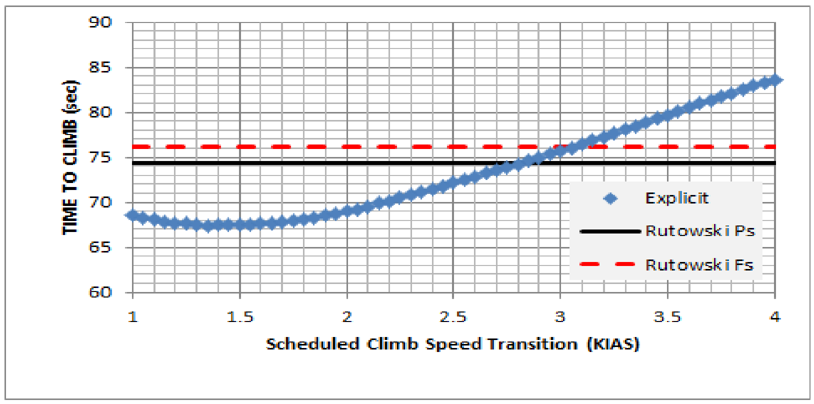

Figure 13 – Time to Climb X-15 Rocketplane configuration

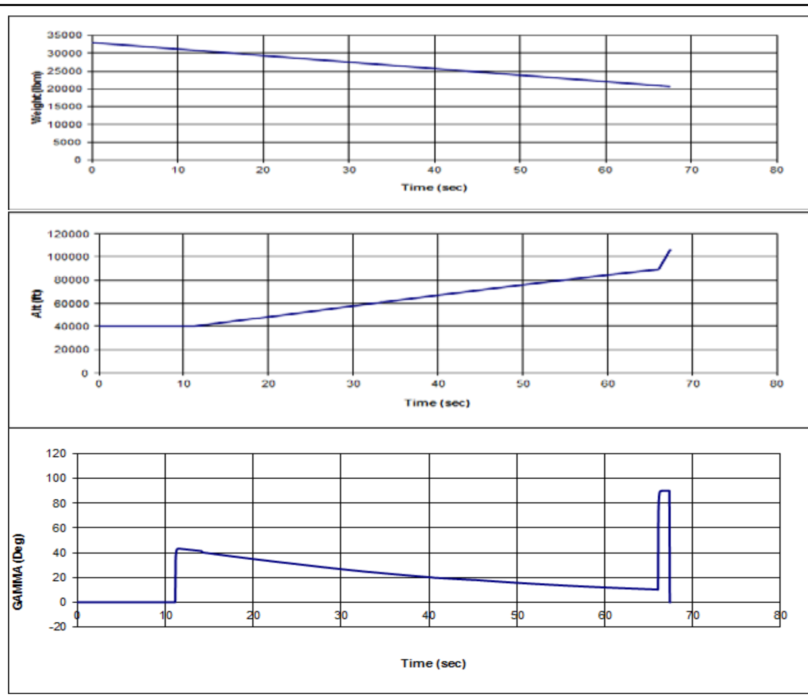

Figure 14 – Flight path X-15 Rocket Plane configuration

Approximately 11 seconds after ignition, the aircraft begins a sharp climb at an initial flight path angle of ~40^o. Once the aircraft attains its terminal velocity of Mach 4.5, it transitions into a constant Mach number climb. At this point, it has burned off enough fuel so that thrust equals or exceeds the remaining weight. Under these circumstances, the aircraft attains a purely ballistic, vertical flight path (90^o flight path angle) trajectory.

VI. Conclusions

The Rutowski method for determining explicit climb and ascent trajectories provides a good starting point for moderately powered aircraft, but performed poorly for very high thrust-to-weight rocket planes that burn a significant portion of their launch mass throughout flight while attaining vertical or near vertical ascent trajectories. As such, it is understandable why programs such as POST and OTIS remain popular for trajectory optimization. At the same time, it is clear that explicit, as opposed to implicit, state variable simulations are suitable to develop optimized trajectories.

While Rutowski's methods are useful to provide insight, they do not define truly "optimal" trajectories for high performance aircraft. It appears that the simplifications inherent in the work-energy theorem derived basic performance equations (flight at small angles of attack, thrust vector is aligned with drag, climb at small flight path angles (i.e. lift is aligned to oppose weight) and climb speed schedule invariant with changes in aircraft weight, fundamentally detract from the veracity of the general method.

At the same time, note the direct utility of specific excess power (*Ps*) as a trajectory shaping screening metric. Climb performance is directly attributable to the magnitude of *Ps*. Fuel specific energy, *Fs*, remains a useful screening metric. These studies demonstrated that in a comparison between two aircraft of otherwise identical weight and wing reference area, the aircraft with greater *Fs* tends to use less fuel in its climb to speed and altitude.

This effect appears to be more related to the time-to-climb attributes of *Ps* rather than the something otherwise intrinsic to *Fs*. Because *Ps* (climb rate) is proportional to specific excess thrust (*SET=(T-D)/W*), fuel flow is primarily a function of total thrust, and aerodynamic drag is a non-negligible fraction of overall thrust, an increase in thrust leads to magnified increase in climb performance. In other words, although fuel flow rates increase in rough proportion to the increase in engine size, the time for which the higher fuel flow is required (the time-to-climb) decreases disproportionately faster. The end result: for all other attributes held constant, more powerful engines burn less fuel during climb than weaker engines because marginal increases in thrust may significantly shorten the overall time to climb.

Ultimately, the true optimal trajectory should be found using a multi-disciplinary-optimization (MDO) approach involving a detailed exploration of all possible speed / altitude schedules using quality aerodynamic and propulsive data.

Acknowledgements

Arizona State University performed this unfunded study using publicly available information regarding the geometry and propulsion system performance of the Airbus A320 and North American X-15 aircraft. Thanks to Phoenix Integration for generous support of ModelCenter licenses. Further thanks to Wolverine Ventures for assistance with NPSS turbofan engine models. I'd also like to express special thanks to Gaines Gibson, M.S. Candidate at ASU, for his assistance in preparing the X-15 aerodynamic and propulsion database used in Section V.

References

[1] Rutowski, E.S., "Energy Approach to the General Aircraft Performance Problem," Journal of the Aeronautical Sciences, Vol. 21, No. 3, 1954, pp. 187-195

[2] Hargraves, C. R., and Paris, S. W., "Direct Trajectory Optimization Using Nonlinear Programming and Collocation ," AIAA Journal of Guidance, Control, and Dynamics, Vol. 10, No. 4, 1987, pp. 338-342.

[3] Brauer, G.L., Cornick, D.E. and Stevenson, R. "Capabilities and Applications of the Program to Optimize Simulated Trajectories (POST)," NASA CR-2770, Feb 1977

[4] *Jet Transport Performance Methods*, Boeing Flight Operations Engineering Training Document D6-1420, 7th Edition, Boeing, Seattle, WA, May 1989
[5] Feagin, R. C., and Morrison,W. D., “Delta Method, An Empirical Drag Buildup Technique,” Lockheed-California Co., Rept. LR-27975-VOL-1, 1978.
[6] NPSS, Numerical Propulsion System Simulation, Software Package, Ver. 2.3.0.1, Ohio Aerospace Institute, Cleveland, OH, 2010.
[7] 14 CFR 91.117 (2015) (Aircraft Speed)
[8] Torenbeek, E., “Optimum Cruise Performance of Subsonic Transport Aircraft," Tech. Rep. LR-787, TU Delft, Faculty of Aerospace Engineering, 1995..
[9] Takahashi, T.T., "Aircraft Concept Design Performance Visualization Using an Energy-Maneuverability Presentation," AIAA 2012-5704, 2012.
[10] German, B.J., Patterson, M.D. and Takahashi, T.T., "Reachability of Optimal Cruise Operating Points: Implications for Aircraft Design," AIAA 2012-1036, 2012
[11] Jenkins, D.R. and Landis, T.R., Hypersonic: The Story of the North American X-15, Specialty Press, North Branch, MN, 2003.
[12] “X-15 Research at the Edge of Space,” NASA EP-9, (1964).
[13] Franklin, A.E., and Lust, R.M., “Investigation of the Aerodynamic Characteristics of a 0.067-Scale Model of the X-15 Airplane (Configuration 3) at Mach Numbers of 2.29, 2.98, and 4.65,” NASA TM-X-38, Langley Research Center, Nov 1958
[14] Saltzman, E.J., “Preliminary Full-Scale Power-Off Drag of the X-15 Airplane for Mach Numbers from 0.7 to 3.1,” NASA TM-X-430, Flight Research Center, December 1960.
[15] Maher, J.F, Ottinger, C.W., and Capasso, V.N., “YLR99RM-1 Rocket Engine Operating Experience in the X-15 Aircraft,” NASA TN-D-2391, July 1964.
[16] McBride, B.J., and Gordon, S., “Computer Program for Calculation of Complex Chemical Equilibrium Compositions and Applications,” NASA RP-1311, June 1996.
[17] Mattingly, J.D., Heiser, W.H., and Pratt, D.T., Aircraft Engine Design,”2nd Edition, AIAA Education Series, Reston, Virginia, 2002

ERRATA

[18] Gibson, G.S. and Takahashi, T.T., “Optimal Suborbital Trajectories for Winged Rocket Planes Using Explicit Simulation,” M.S. Applied Project Report, School for Engineering of Matter Transport and Energy, Arizona State University, Tempe, AZ, 2015.